Nonlinear Relay Model for Post-Stall Oscillations

Arthur L. Schoenstadt*
Naval Postgraduate School, Monterey, Calif.

This paper considers an analytic treatment of divergent oscillations in the post-stall region for a general class of aircraft. A limited, numerical investigation, on a single aircraft, has shown that a sufficiently large negative lift slope can lead to these oscillations. Our investigation models the post-stall behavior in a general class of aircraft, under the hypothesis that, if the slope of the lift curve is sufficiently negative then the aircraft will see an essentially instantaneous loss of lift, which can be modeled by the introduction of a hypothetical relay. Linearity assumptions on the other terms, together with conditions on the magnitude of various coefficients, lead to a system of coupled, constant coefficient, first-order differential equations, with a forcing term characterized by a jump discontinuity. Analysis of this system yields a necessary and sufficient condition for the existence of a limit cycle, and transcendental equations predicting the period of this cycle. These conditions give predictions in excellent agreement with the results of the numerical investigation.

Nomenclature

$\bar{c}$ = mean aerodynamic chord (MAC)
C_D = drag coefficient
C_L = lift coefficient
C_M = pitching moment coefficient
g = gravitation acceleration
I_y = moment of inertia about c.g.
m = mass
q = $\frac{1}{2}\rho v^2$
S = wing reference area
T = thrust
u = velocity component along thrust line ($= v\cos\alpha$)
v = velocity along flight path
v_o = velocity at trim configuration
w = velocity component normal to thrust line ($= v\sin\alpha$)
α = angle of attack
α_o = angle of attack at trim configuration
δ_e = elevator deflection angle
θ = pitch angle
θ_o = pitch angle at trim configuration
ρ = density of air
$\Delta\alpha$ = $\alpha-\alpha_o$
$\Delta\theta$ = $\theta-\theta_0$
$(\cdot)$ = $d(\ )/dt$

I. Introduction

CONSIDERABLE literature exists describing the static characteristics of aircraft near, or at, stall, including detailed analyses of stall tendencies. However, there appears to be little information on, or analytic treatment of, aircraft dynamics in the region around stall, and especially post-stall time histories in which divergent oscillations arise. The latter phenomenon is quite interesting, since experienced pilots apparently are familiar with the "rocking chair" or "porpoising" stall, where the aircraft, with constant elevator angle, alternately enters stall, then recovers, leading to a vertical oscillation of the aircraft nose about some point.

Normally we define the airplane stall angle as that angle where the vehicle's trimmed lift curve (C_L vs α) has a global maximum. It is well known that the lift curve then exhibits a negative slope for some range of α above the stall angle. Therefore, we shall also use here α_c, the stall break angle, defined as that angle where the lift curve has maximum negative slope (Fig. 1). There is a paucity of information on the nature of the lift curve in the post-stall or stall break region, since experimental wind tunnel data has usually been smoothed through this region based on engineering intuition. In addition, actual treatment to define the stall break for a physical aircraft is difficult since model data are subject to scaling difficulties and aircraft parameter identification in the nonlinear region is limited as present.

In his thesis, Frederiksen[1] considered the problem of divergent oscillations and limit cycles in this region. His linear analysis was able to show, numerically for a single aircraft, that a sufficiently large negative slope in C_L in this region led to roots for the characteristic equation which had positive real parts (i.e., exponentially growing). This behavior is, of course, transitory, and disappears by the time the aircraft returns to a configuration where the lift slope is positive. However, it did provide an insight into the mechanism that might cause these oscillations. Furthermore, he was able to simulate numerically time histories in which a "rocking chair" stall did occur. However, due to the numerical nature of his work and his concentration on a single aircraft, his results are not readily extendible, or suitable for general analysis.

This investigation attempts to analytically model the post-stall behavior in a general class of aircraft. Our main hypothesis is that, if the slope of the lift curve is sufficiently negative in the region beyond the stall break, then the aircraft will behave as if it sees a sharp, essentially instantaneous loss of lift. If this is the case, then the lift curve can be more conveniently modeled in this region by the introduction of a hypothetical "relay" acting at the stall break angle. We assume that, except for this nonlinearity, C_L, C_M and C_D can be adequately approximated by linear functions. Those assumptions, together with conditions on the magnitude of various coefficients, lead to a system of coupled, constant

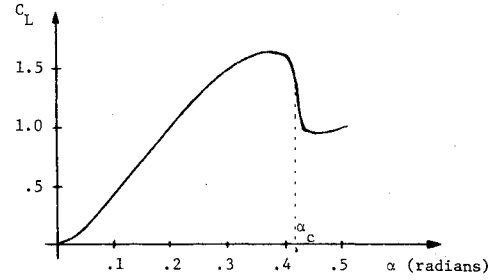

Fig. 1 Typical C_L vs α curve.

Received October 29, 1973; revision received October 29, 1974. This project was supported by the Foundation Research Program, Naval Postgraduate School. The author is indebted to L. V. Schmidt for many helpful discussions.

Index categories: Aircraft Aerodynamics (including Component Aerodynamics); Aircraft Handling, Stability, and Control.

*Assistant Professor, Department of Mathematics.

coefficient, first-order differential equations, with a forcing term which has a jump discontinuity. Analysis of this system yields a necessary and sufficient condition for the existence of a limit cycle, and transcendental equations predicting the period of this cycle. These conditions are then applied to the case considered by Frederiksen, and it is shown our model yields excellent agreement with his results.

II. Derivation of the Model

The aircraft, assumed to be in longitudinal flight, will be described by means of the standard coordinate system shown in Fig. 2. In this system, the equations of motion become

$$\dot{u}=\{T+qS[C_l \sin\alpha - C_D\cos\alpha]\}/m - g\sin\theta - w\dot{\theta} \tag{1}$$

$$\dot{w}=-qS[C_L\cos\alpha + C_D\sin\alpha]/m + g\cos\theta + u\dot{\theta} \tag{2}$$

$$\ddot{\theta}=(qS\bar{c}/I_y)C_M \tag{3}$$

and

$$\dot{\alpha}=\{-\dot{u}\sin\alpha + \dot{w}\cos\alpha\}/v \tag{4}$$

In most applications where the range of the variables is small, the coefficients in this nonlinear system, although themselves generally nonlinear, can be adequately approximated by linear functions. As is obvious from Fig. 1, this is not the case for C_L in the neighborhood of the stall break.

The model developed here describes motion in a small region about the stall break. The aircraft considered is trimmed initially for constant attitude and angle of attack, and the elevator angle and thrust, denoted by δ_e and T, are assumed held constant throughout. The velocity in trim configuration is denoted v_o, and since Frederiksen's results do not show a significant variation in v compared to that in α and θ during limit cycles, we assume $v=v_o$. Perturbations off the trim configuration and their derivatives are represented in the usual manner, e.g., $\Delta\alpha=\alpha-\alpha_o$, and $\Delta\dot{\alpha}=(d/dt)(\Delta\alpha)=\dot{\alpha}$, etc.

The key ingredient of this investigation is modeling C_L at the stall break. Reference to Fig. 1 indicates that, if the negative slope in the region past the stall break is sufficiently steep, then an aircraft entering this region experiences an almost instantaneous loss in lift. This is essentially equivalent to the action of a hypothetical "relay" in the lift curve function C_L. Thus, we shall model the lift curve as:

$$C_L=C_{L0}+C_{L\delta_e}\delta_e+(\bar{c}/2v_o)C_{L\dot{\theta}}\Delta\dot{\theta} + C_{L\alpha_c}\Delta\alpha - C_{L\Delta}\mathrm{sgn}\,(\alpha-\alpha_c) \tag{5}$$

where $\mathrm{sgn}(x)=|x|/x$, $x\neq 0$, $\mathrm{sgn}(0)=0$, and α_c denotes the stall break angle. Figure 3 shows a sketch of a C_L curve generated by Eq. (5) superimposed on the C_L curve from Fig. 1.

As noted, we will approximate C_M and C_D linearly, so that

$$C_D=C_{D0}+C_{D\alpha}\Delta\alpha \tag{6}$$

and

$$C_M=-C_{M0}-C_{M\alpha}\Delta\alpha-(\bar{c}/2v_o)C_{M\dot{\theta}}\Delta\dot{\theta} - (\bar{c}/2v_o)C_{M\dot{\alpha}}\Delta\dot{\alpha}-C_{M\delta_e}\delta_e \tag{7}$$

(At stall, aerodynamic load distribution and intensity may change substantially. This somewhat limits the generality of our model, based as it is on linearity of C_M and C_D in this region. However, in those cases where C_M and C_D cannot be satisfactorily approximated by linear terms, but can be by linear terms plus a $\mathrm{sgn}(\alpha-\alpha_o)$ term, a minor modification in this model should yield valid results.) Note, to facilitate analysis, we have assigned algebraic signs so that, in normal cases, all coefficients are positive.

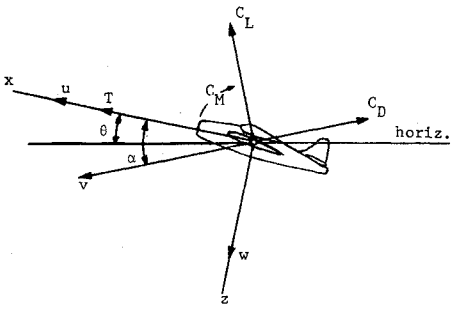

Fig. 2 Aircraft coordinate system.

Now if $\dot{u}$ and $\dot{w}$ which appear in Eq. (4) are replaced by their equivalent expression in terms of Eqs. (1) and (2), and the derivatives are replaced by the equivalent derivatives of the perturbed quantities, we can reduce Eq. (3) and (4) to

$$\Delta\dot{\alpha}=-(T/mv_o)\sin(\alpha_o+\Delta\alpha)-(qS/mv_o)C_L + (g/v_o)\cos(\theta_o-\alpha_o+\Delta\theta-\Delta\alpha)+\Delta\dot{\theta} \tag{8}$$

and

$$\Delta\ddot{\theta}=(qS\bar{c}/I_y)C_M \tag{9}$$

Then, under the assumption that $\Delta\alpha$ and $\Delta\theta$ are small, the trigonometric terms in Eq. (8) can be expanded, neglecting second-order and higher terms, after which the defining equation for C_L can be used to reduce Eq. (8) to:

$$\Delta\dot{\alpha}=\{-\frac{T}{mv_o}\sin\alpha_o-\frac{qS}{mv_o}[C_{L0}+C_{L\delta_e}\delta_e] + \frac{g}{v_o}\cos(\theta_o-\alpha_o)\}+\{\frac{g}{v_o}\sin(\theta_o-\alpha_o)-\frac{T}{mv_o}\cos\alpha_o - \frac{qS}{mv_o}C_{L\alpha_c}\}\Delta\alpha-\{\frac{g}{v_o}\sin(\theta_o-\alpha_o)\}\Delta\theta + \{1-\frac{qS\bar{c}}{2mv_o^2}C_{L\dot{\theta}}\}\Delta\dot{\theta}+\frac{qS}{mv_o}C_{L\Delta}\mathrm{sgn}[\Delta\alpha-(\alpha_c-\alpha_o)] \tag{10}$$

Now, using this expression to replace $\Delta\dot{\alpha}$ in Eq. (7), the equation for C_M, and substituting the resulting expression into Eq. (9), yields

$$\Delta\ddot{\theta}=\frac{qS\bar{c}}{I_y}\Big[\{-C_{M0}-C_{M\delta_e}\delta_e-\frac{\bar{c}}{2v_o}C_{M\dot{\alpha}} \times[-\frac{T}{mv_o}\sin\alpha_o-\frac{qS}{mv_o}(C_{L0}+C_{L\delta_e}\delta_e) \frac{g}{v_o}\cos(\theta_o-\alpha_o)]\}-\{C_{M\alpha}+\frac{\bar{c}}{2v_o}C_{M\dot{\alpha}}[\frac{g}{v_o}\sin(\theta_o-\alpha_o) - \frac{T}{mv_o}\cos\alpha_o-\frac{qS}{mv_o}C_{L\alpha_c}]\}\Delta\alpha + \{\frac{g\bar{c}}{2mv_o^2}C_{M\dot{\alpha}}\sin(\theta_o-\alpha_o)\}\Delta\theta - \frac{\bar{c}}{2v_o}\{C_{M\dot{\theta}}+C_{M\dot{\alpha}}[1-\frac{qS\bar{c}}{2mv_o^2}C_{L\dot{\theta}}]\}\Delta\dot{\theta} - \frac{qS\bar{c}}{2mv_o^2}C_{M\dot{\alpha}}C_{L\Delta}\mathrm{sgn}(\Delta\alpha-(\alpha_c-\alpha_o))\Big] \tag{11}$$

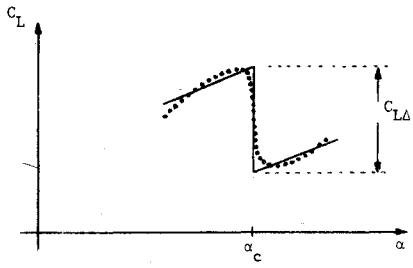

Fig. 3 Approximation to C_L: .... ≡ actual C_L;—≡ given by Eq. (5).

Equations (10) and (11) then describe our model.

In practice, many of the terms which appear in Eqs. (11) and (12) are negligible. Calculations, using representative values, will show for many, if not all cases, little is lost by assuming

$$\frac{qS\bar{c}}{2mv_o^2} C_{L\dot{\theta}} \ll 1, \quad \frac{\bar{c}}{2v_o} C_{M\dot{\alpha}} \ll 1$$

and also that

$$\frac{g}{v_o} \sin(\theta_o - \alpha_0) - \frac{T}{mv_o} \cos \alpha_o - \frac{qS}{mv_o} C_{L\alpha_c} \ll 1$$

and

$$\frac{g}{v_o} \sin(\theta_o - \alpha_o) \ll 1$$

Now, our assumption that the aircraft was trimmed at α_o, θ_o implies that all time derivatives vanish there. Thus, imposition of the trim condition to Eqs. (10) and (11) will yield two additional relations, which can then be incorporated back into Eqs. (10) and (11) to simplify the original equations. Finally, incorporating the assumption on small values made above results in the equations:

$$\Delta\dot{\alpha} = \Delta\dot{\theta} + \frac{qS}{mv_o} C_{L\Delta} \times \{\operatorname{sgn}(\Delta\alpha - (\alpha_c - \alpha_o)) + \operatorname{sgn}(\alpha_c - \alpha_o)\} \tag{12}$$

and

$$\Delta\ddot{\theta} = -\frac{qS\bar{c}}{I_y} C_{M\alpha} - \frac{qS\bar{c}^2}{2v_o I_y} \{C_{M\dot{\theta}} + C_{M\dot{\alpha}}\} \Delta\dot{\theta} - \frac{(qS\bar{c})^2}{2mI_y v_o^2} C_{M\dot{\alpha}} C_{L\Delta} \times \{\operatorname{sgn}(\Delta\alpha - (\alpha_c - \alpha_o)) + \operatorname{sgn}(\alpha_c - \alpha_o)\} \tag{13}$$

We now define the quantities β, ω, a, and ζ by

$$\frac{qS\bar{c}}{I_y} C_{M\alpha} = (\beta^2 + \omega^2) > 0 \tag{14a}$$

$$\frac{qS\bar{c}^2}{2v_o I_y} \{C_{M\dot{\theta}} + C_{M\dot{\alpha}}\} = 2\beta > 0 \tag{14b}$$

$$\frac{qS}{mv_o} C_{L\Delta} = a > 0 \tag{14c}$$

and

$$\frac{qS\bar{c}^2}{2v_o I_y} C_{M\dot{\alpha}} = \zeta > 0 \tag{14d}$$

Since it becomes important in our later discussion, note here that the quantity:

$$(2\beta - \zeta) = \frac{qS\bar{c}^2}{2v_o I_y} C_{M\dot{\theta}} > 0$$

Thus our model for the flight dynamics of an aircraft, trimmed for longitudinal flight at an angle of attack near the stall break angle, becomes:

$$\Delta\dot{\alpha} = \Delta\dot{\theta} + a\{\operatorname{sgn}(\Delta\alpha - (\alpha_c - \alpha_o)) + \operatorname{sgn}(\alpha_c - \alpha_o)\} \tag{15}$$

$$\Delta\ddot{\theta} = -(\beta^2 + \omega^2)\Delta\alpha - 2\beta\,\Delta\dot{\theta} - \zeta a \times \{\operatorname{sgn}(\Delta\alpha - (\alpha_c - \alpha_o)) + \operatorname{sgn}(\alpha_c - \alpha_o)\} \tag{16}$$

(Note that Eqs. (15) and (16) describe a simultaneous first-order system in $\Delta\alpha$ and $\Delta\dot{\theta}$. Since the original system [Eqs. (1-4)] was equivalent to a first-order system in four variables, α, θ, $\dot{\theta}$, and v, our model will obviously not describe the full range of dynamics. However, we will show that it does appear to predict the known limit cycle behavior. In essence, what we are doing in Eqs. (15) and (16) is basing our analysis on the influence of the stall break on the short period mode of the aircraft, and neglecting the long period mode. Furthermore, the mathematical advantages of dealing with a two variable system are enormous.)

III. Flight with Trim at the Stall Break Angle

We limit our investigation of the model described by Eq. (15) and (16) to the case $\alpha_c = \alpha_o$, that is the aircraft is trimmed for flight at the stall break. Then since $\alpha_c - \alpha_o = 0$, the second sgn function in both Eqs. (15) and (16) disappears. If we let $x_1 = \Delta\dot{\theta}$ and $x_2 = \Delta\alpha$, our system reduces to

$$\dot{x}_1 = -2\beta x_1 - (\beta^2 + \omega^2)x_2 - \zeta a \operatorname{sgn} x_2$$

$$\dot{x}_2 = x_1 + a \operatorname{sgn} x_2 \tag{17}$$

A. Geometric Behavior of Solutions

Consider the analytic behavior of this system in the (x_1, x_2) plane. The line $x_2 = 0$, which we refer to as the switching line, divides the plane into two regions where, separately, the equations are linear, constant coefficient, and homogeneous. A key observation is that the right-hand sides of both equations in (17) are odd functions of x_1 and x_2, and hence solution trajectories to this system appear in pairs which are symmetric with respect to the origin. Thus, we need direct our attention solely to the region $x_2 \geq 0$, and draw any needed information about $x_2 < 0$ by symmetry arguments.

The critical (rest) points of this system, i.e., the points where $\dot{x}_1 = \dot{x}_2 = 0$, in the region $x_2 \geq 0$, are given by $x_1 = x_2 = 0$ and

$$x_1 = -a, \; x_2 = \frac{(2\beta - \zeta)}{(\beta^2 + \omega^2)} a$$

(The second point has a symmetric image in $x_2 < 0$.) The fact that $(2\beta - \zeta) > 0$ guarantees the critical point in $x_2 > 0$ actually exists. The critical point at the origin is unstable, due to the sgn term in Eq. (17). However, the homogenous part of Eq. (17) has a characteristic polynomial $\lambda^2 + 2\beta\lambda + (\beta^2 + \omega^2)$ whose roots must have negative real parts according to our definition of β and ω in Eq. (14). Hence, the two critical points not at the origin are locally asymptotically stable. (That is, small perturbations off them decay back.)

B. Conditions for a Limit Cycle

From the previous stability discussion, any limit cycle trajectory must pass through the switching line, and be symmetric with respect to the origin. Thus, any arc of the limit cycle in the region $x_2 > 0$, must originate on the switching line

at the point $(x_1^*,0)$, and, after a half-period, must terminate at the point $(-x_1^*,0)$. Thus, if we denote the half-period by τ, a necessary condition for a limit cycle period 2τ is:

$$x_1(0) = -x_1(\tau)$$

$$x_2(0) = x_2(\tau) = 0 \tag{18}$$

(This situation is represented in Fig. 4.)

It is easily shown that in the region $x_2 > 0$ the solution to Eq. (17) is given by

$$x_1(t) = -c_1 e^{-\beta t}(\beta \cos \omega t + \omega \sin \omega t) + c_2 e^{-\beta t}(\omega \cos \omega t - \beta \sin \omega t) - a \tag{19}$$

and

$$x_2(t) = c_1 e^{-\beta t} \cos \omega t + c_2 e^{-\beta t} \sin \omega t + \frac{(2\beta - \zeta)}{(\beta^2 + \omega^2)} a \tag{20}$$

(These simply represent arcs of decaying counterclockwise spirals centered at the critical point in the upper half plane.) Since the critical point is asymptotically stable, there must be some curves in the region which never exit it, but decay down to the critical point. Other curves will at some time exit the region. Finally, since any trajectory interesecting the line $x_1 = -a$ in the region $x_2 < 0$ has a horizontal slope at the point of intersection [see Eq. (17)], the boundary between the decaying curves and those that exit to $x_2 < 0$ must just be that curve which terminates at $(-a,0)$. (This curve is labeled in Fig. 5.)

But the time interval represented by a trajectory in the region $x_2 > 0$ is a function of the counterclockwise angle (as seen from the critical point) between the initial point $[x_1(0), 0]$, and the point at which the trajectory first touches the switching line again. Thus, any curve which represents a half-period of a limit cycle must spend less time in $x_2 > 0$ than τ_o, where τ_o is the time represented by the curve (*) in Fig. 5. Thus τ satisfies

$$\pi/\omega < \tau < \tau_o$$

where

$$x_1(\tau_o) = -a$$

$$x_2(0) = x_2(\tau_o) = 0 \tag{21}$$

Conditions (18) and (21) now provide both the necessary and sufficient conditions for existence of a limit cycle of period 2τ.

Applying the conditions given in Eq. (18) to the solutions (19) and (20) yield three equations involving c_1, c_2 and τ. Solving two of these for c_1 and c_2 in terms of τ, and substitution of these expressions into the third, followed by simplification shows that Eq. (18) reduces to

$$\sinh \beta\tau = -\frac{(\omega^2 + \beta\zeta - \beta^2)}{\omega(2\beta - \zeta)} \sin \omega\tau \tag{22}$$

A similar application of the definition of τ_o in Eq. (21) to the solutions given by Eqs. (19) and (20) yields

$$\omega \cos \omega\tau_o - \beta \sin \omega\tau_o = \omega e^{-\beta\tau_o} \tag{23}$$

In view of our earlier comments, τ_o is defined as the smallest positive solution of Eq. (23). Mathematically, then we can summarize our results as follows.

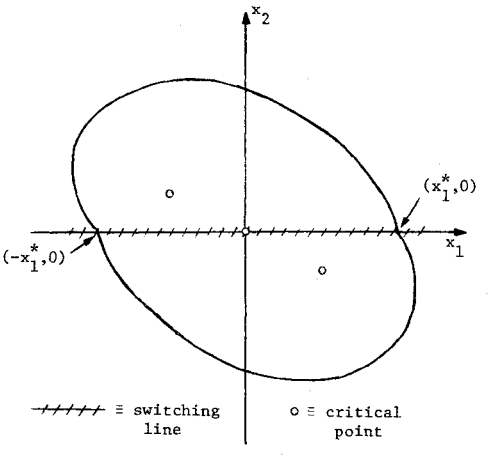

Fig. 4 Limit cycle necessary condition.

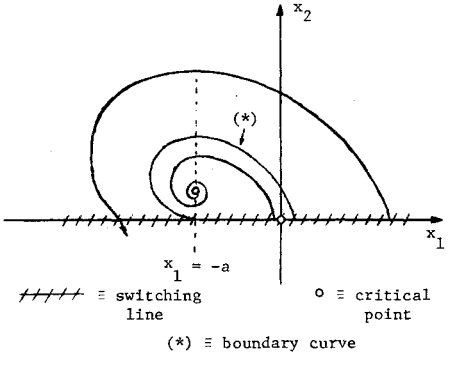

Fig. 5 Boundary curve in $x_2 > 0$.

Table 1 Parameters for F-94[a]

ρ	$= 2.38 \times 10^{-3}$ slugs/ft^3	$\bar{c}$	$= 6.40$ ft
m	$= 384$ slugs	Iy	$= 2.65 \times 10^4$ slug ft^2
S	$= 239.0$ ft^2		
C_{L0}	$= 1.440$	$C_{L\delta_e}$	$= 0.43$
$C_{L\alpha_c}$	$= 0.30$	$C_{L\dot{\theta}}$	$= 10^{-5}$
$C_{L\Delta}$	$= 0.05$		
C_{M0}	$= 0.15$	$C_{M\dot{\alpha}}$	$= 4.27$
$C_{M\alpha}$	$= 1.54$	$C_{M\delta_e}$	$= 0.88$
$C_{M\dot{\theta}}$	$= 8.16$		
θ_o	$= 0.099$	v_o	$= 169$ fps
α_o	$= 0.41$ rad	T	$= 0.0$ lb
α_c	$= 0.41$ rad		

[a] Values used by Frederiksen.[1]

Theorem: The system Eq. (17) will have a limit cycle of period 2τ if and only if τ satisfies Eq. (22) and

$$\pi/\omega < \tau < \tau_0$$

where τ_o is the smallest positive solution of Eq. (23).

C. Example—The Case Considered by Frederiksen[1]

To determine validity of the predictions of this model, consider the case used by Frederiksen.[1] Table 1 shows the table of values appropriate to this case, which describes the F-94, a straight wing, single engine jet. The value of the coefficients appropriate to the linearized differential equations were computed and are shown in Table 2. Note that our assumptions on small size of certain coefficients seem valid. Using the values

Table 2 Coefficients for the differential equations based on parameters in Table 1

$$\frac{qS\bar{c}}{2v_o^2} C_{L\dot{\theta}} = 2.4 \times 10^{-8}, \quad \frac{\bar{c}}{2v_o} C_{Mq} = 0.081$$

$$\frac{g}{v_o} \sin(\theta_o - \alpha_o) = -0.058$$

$$\frac{g}{v_o} \sin(\theta_o - \alpha_o) - \frac{T}{mv_o} \cos \alpha_o - \frac{qS}{mv_o} C_{L\alpha_c} = -0.096$$

$$\frac{qS\bar{c}}{I_y} C_{M\alpha} = (\beta^2 + \omega^2) = 3.00^a$$

$$\frac{qS\bar{c}^2}{2v_o I_y} \{C_{M\dot{\theta}} + C_{M\dot{\alpha}}\} = 2\beta = 0.46^a$$

$$\frac{qS}{mv_o} C_{L\Delta} = a = 6.3 \times 10^{-3}$$

$$\frac{qS\bar{c}^2}{2v_o I_y} C_{M\dot{\alpha}} = \zeta = 0.16$$

$$(2\beta - \zeta) = 0.30 > 0$$

[a]Implies $\beta = 0.23$, $\omega = 1.72$.

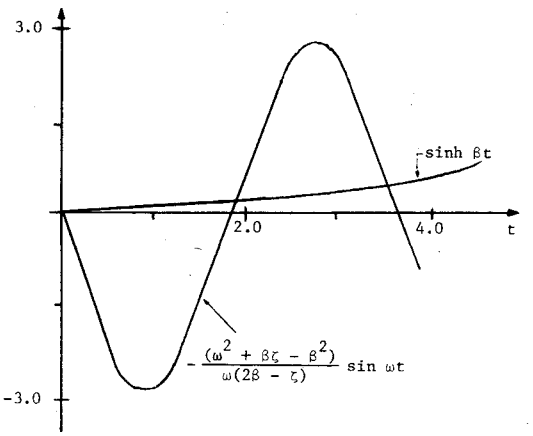

Fig. 6 Graphical solution of Eq. (22).

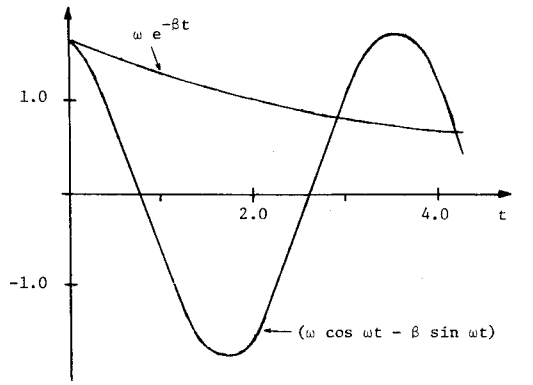

Fig. 7 Graphical solution of Eq. (23).

of β, ω and ζ so computed, Eqs. (22) and (23) were graphically and numerically solved, and are graphically portrayed in Figs. 6 and 7, respectively. There are obviously two solutions of Eq. (22) in the region $\pi/\omega < \tau < 2\pi/\omega$: $\tau = 1.87$ and $\tau = 3.56$. But τ_o, defined as the first positive intersection of the curves in Fig. 7, is given by $\tau_o = 3.10$. Thus, only the lower value of τ satisfies the requirement $\pi/\omega < \tau < \tau_o$ and there will be exactly one limit cycle, with period $2\tau = 3.74$ sec. Computing c_1 and c_2, which we commented could be determined in terms of τ,

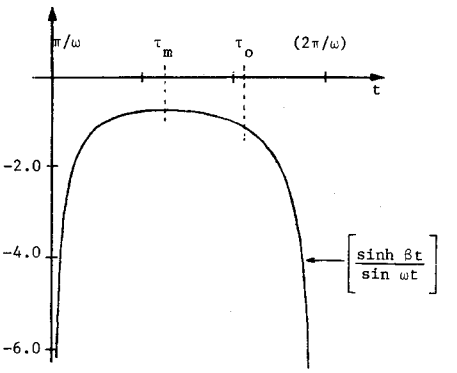

Fig. 8 Typical graph of $G(t)$.

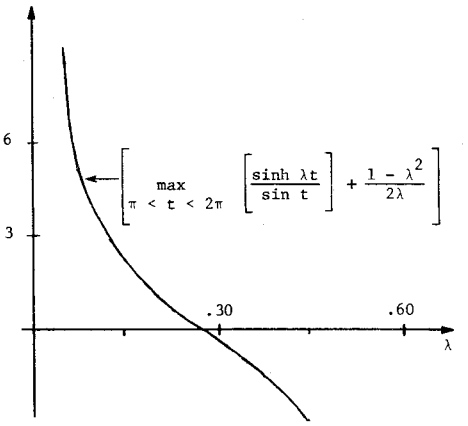

Fig. 9 Graphical solution of Eq. (28).

and using the values to describe $x_2(t) = \Delta\alpha(t)$ as given by Eq. (20), leads to an amplitude for this limit cycle of $\Delta\alpha_{max} = 0.018$ rad $\doteq 1^0$. These values are in very good agreement with those obtained by Frederiksen, which were $2\tau = 3.77$ sec, $\Delta\alpha_{max} = 0.020$ rad.

D. Additional Comment

We shall make on other fairly important observation on the mathematical nature of Eqs. (22) and (23). Note that Eq. (22) is equivalent to

$$\frac{\sinh \beta\tau}{\sin \omega\tau} = -\frac{\omega^2 + \beta\zeta - \beta^2}{\omega(2\beta - \zeta)} \tag{24}$$

Now since $(2\beta - \zeta) > 0$, the region of interest for this eqation is $\pi/\omega < \tau < 2\pi/\omega$. We denote

$$G(t) = \sinh \beta t / \sin \omega t \tag{25}$$

$G(t)$ is negative in the interval, and becomes vertical as t approaches $(\pi/\omega)^+$ and $(2\pi/\omega)^-$. A straightforward analysis of the properties of its derivative, particularly the algebraic sign of its numerator (the denominator being a square), shows that $G(t)$ is monotonic increasing up to a unique maximum, which occurs at some point τ_m, then monotonically decreasing for the remainder of the interval. [Figure 8 shows a general form for $G(t)$.] Since $G(t)$ has these monotonicity properties, the relative locations of τ_o and τ_m can be determined by considering $(dG/dt)(\tau_o)$. The derivative is evaluated by replacement of the $\beta \sin \omega\tau_o$ term by Eq. (23), and simplification, yielding $(dG/dt)(\tau_o) < 0$, i.e., $G(t)$ is decreasing at τ_o, and so by our earlier comment, $\tau_m < \tau_o$.

But observe that the right-hand side of Eq. (24) is independent of τ. Thus, since Eq. (22) and (24) are equivalent, a necessary and sufficient condition for Eq. (22) to have a solution, based on our analysis of $G(t)$, is

$$\max_{\pi/\omega < t < 2\pi/\omega} \left[\frac{\sinh \beta t}{\sin \omega t}\right] \geq -\frac{\omega^2 + \beta\zeta - \beta^2}{\omega(2\beta - \zeta)} \tag{26}$$

Finally since $G(\pi^+/\omega) = -\infty$ and $\tau_m < \tau_o$, then if Eq. (26) is satisfied, then there must be a $\tau < \tau_m < \tau_o$ such that

$$\frac{\sinh \beta\tau}{\sin \omega\tau} = -\frac{\omega^2 + \beta\zeta - \beta^2}{\omega(2\beta - \zeta)}$$

Then this τ satisfies Eq. (22) and (23), and so generates a limit cycle. Thus, Eq. (26) expresses a necessary and sufficient condition for existence of a limit cycle in this model. This is expressed by the following theorem.

Theorem: The system (17), where $(2\beta - \zeta) > 0$, will have a limit cycle solution if and only if Eq. (26) is satisfied.

Observe that, with the substitution $\lambda = \beta/\omega > 0$, and $\eta = \zeta/\omega > 0$, the necessary and sufficient condition becomes

$$\max_{\pi < t < 2\pi} \left[\frac{\sinh \lambda t}{\sin t} \right] \geq -\frac{1 + \eta\lambda - \lambda^2}{(2\lambda - \eta)} \tag{27}$$

(the left-hand side of which is clearly a function of λ only.) Since $(2\beta - \zeta) > 0$, then $(2\lambda - \eta) > 0$, or $0 < \eta < 2\lambda$. Straightforward analysis can show the right-hand side of Eq. (27) has its maximum value at $\eta = 0$. Thus, clearly a *sufficient* condition for Eq. (27) to be satisfied, and hence for a limit cycle to exist, is,

$$\max_{\pi < t < 2\pi} \left[\frac{\sinh \lambda t}{\sin t} \right] \geq \frac{\lambda^2 - 1}{2\lambda} \tag{28}$$

In Fig. 9 we plot the function

$$\max_{\pi < t < 2\pi} \left[\frac{\sinh \lambda t}{\sin t} \right] + \frac{1 - \lambda^2}{2\lambda}$$

for $0 < \lambda < 1$, and observe that Eq. (28) can be satisfied if and only if

$$\lambda \leq 0.280 \tag{29}$$

Thus, Eq. (29) expresses a *sufficient* condition for existence of a limit cycle.

Now if $\lambda \leq 0.280$ and $\beta = \lambda\omega$, we have

$$\omega^2 \leq \omega^2 + \beta^2 = (1 + \lambda^2)\ \omega^2 \leq 1.078\ \omega^2$$

and so we can approximate $\omega \doteq (\omega^2 + \beta^2)^{1/2}$. But then, according to the definitions of Eq. (14), $\lambda = \beta/\omega$ is proportional to

$$\frac{C_{M\dot{\alpha}} + C_{M\theta}}{C_{M\alpha}}$$

and we see our sufficient condition Eq. (29) translates into a statement that $C_{M\dot{\alpha}}$ is somehow small compared to $C_{M\alpha}$. Since $C_{M\alpha}$ is analogous to a spring constant, and $C_{M\theta}$ and $C_{M\dot{\alpha}}$ are damping terms, we can view Eqs. (28) and (29) as saying:

"A sufficient condition for existence of a limit cycle behavior in the presence of a sharp negative lift slope, is that the damping terms in C_M are small relative to the "restoring" term, $C_{M\alpha}$." Clearly this interpretation makes physical "sense."

IV. Summary and Conclusions

In this paper, we have developed and analyzed a simple two-variable model for post-stall time histories in the presence of a sharp lift loss at stall. This model yields a simple necessary and sufficient condition for the occurrence of a limit cycle, i.e., "rocking chair" stall. Furthermore, the model predicts values that are in very close agreement with those obtained from numerical solution of the full, four-dimensional, nonlinear case. Lastly, the model yields physically satisfying information about the important parameters for occurrence of this limit cycle.

References

[1] Frederiksen, J. T., "An Evaluation of the Longitudinal Dynamic Stability of an Aircraft at Stall," M.S. thesis, June 1972, Naval Postgraduate School, Monterey, Calif.